

MOLECULAR STRUCTURE EFFECTS ON DIFFUSION OF CATIONS IN CLAYS

ALANAH FITCH, JOHN SONG, AND JENNY STEIN

Department of Chemistry, Loyola University of Chicago, 6525 N. Sheridan Rd.
Chicago, Illinois 60626

Abstract—The roles of molecular structure and charge are examined in the transport of cations within montmorillonite clay films. The series of $\text{Ru}(\text{NH}_3)_6^{3+}$, $\text{Co}(\text{NH}_3)_3^{3+}$, $\text{Co}(\text{en})_3^{3+}$, $\text{Co}(\text{sep})^{3+}$ and $\text{Co}(\text{bpy})_3^{3+}$ are examined in detail via electrochemical and spectrochemical methods. The electrochemical signal is enhanced both in minimizing the time required to develop the signal and in the magnitude of the signal for $\text{Ru}(\text{NH}_3)_6^{3+}$. In addition, the potential for the observed reduction peak is shifted negative and the current peak associated with reduction disappears with rinsing of the clay film. These observations are characteristic of a compound that is held by simple electrostatic charge characteristics. In contrast, the compounds $\text{Co}(\text{NH}_3)_3^{3+}$, $\text{Co}(\text{en})_3^{3+}$ and $\text{Co}(\text{sep})^{3+}$, while showing rapid and enhanced signal development, eventually evolve a signal that is diminished with respect to the bare electrode, consistent with a hydrophobic mode of retention. The signal for $\text{Co}(\text{bpy})_3^{3+}$ is slow to be observed, is diminished with respect to the bare electrode and is shifted positive in potential, all hallmarks of a strong, non-electrostatic mode of binding within the clay.

Key Words—Clay-modified electrodes, Co complexes, Diffusion, Transport.

INTRODUCTION

Clay containment barriers create a network of fine pores that prevent gravitational flow of water (Goldsmann et al. 1990). When flow of water is restricted, the transport of a pollutant across the barrier is governed by diffusion. Diffusion is expected to be low when the concentration of mobile species is reduced to clay surface adsorption (Mott and Weber 1991; Wang et al. 1991). Under these conditions, predicted times for pollutant breaching a clay barrier are several hundred years. Field trials, however, have shown that some small molecules do not adhere to this behavior and move rapidly through soils (Johnson et al. 1989; Goodall and Quigley 1977; Quigley et al. 1987; Barone et al. 1989; Crooks and Quigley 1989). As a result the mode of diffusive transport of solutes through clay films is of interest. Diffusive transport is also of interest in examining solute access to reactive sites within clay systems and in the rational design of sensors based on clay systems.

In order to study diffusion in clays, we have developed the technique of clay-modified electrodes (CME) where the gradient driving transport is unaffected by hydraulic considerations (Fitch et al. 1988; Fitch and Fausto 1988; Fitch and Edens 1989; Lee and Fitch 1990; Fitch 1990a, 1990b; Wieglos and Fitch 1990; Edens et al. 1991; Fitch and Du 1992; Subramaniam and Fitch 1992; Fitch and Lee 1993; Fitch and Subramaniam 1993; Stein and Fitch 1995; Fitch et al. 1995). In this method, a well-ordered clay gel is formed on a flat glass surface in which a Pt wire is embedded. The clay film is swollen in controlled conditions and then exposed to a solution containing an

electroactive probe molecule. The arrival of the probe molecule at the Pt surface can be monitored by a current associated with the reduction/oxidation of the probe. In the initial phase of filling, the current is directly related to transient diffusion across the film which depends upon both the pore structure of the film and the partition coefficient of the solute into the film. In the final phase of filling, the current is related to an equilibrium diffusion of the solute within the film, which after all sites are filled, depends primarily upon pore structure.

Thus, the pore structure of these thin, small area, films is crucial. We have observed that when an anionic probe molecule, $\text{Fe}(\text{CN})_6^{3-}$, is used the current is diminished when the clay film is collapsed (5 M NaCl) and increased when the clay film is swollen (0.1 M NaCl), suggesting that the limiting step is diffusion through a constricting pore defined by the interlayer region.

Since transport is constrained in at least one point by interlayer transport, in this study, we probe the effect of molecular structure of cationic probes in these small channels. Two extreme types of cationic interaction with the clay are identified and form the ends of a transport continuum. For Case I, the molecule simply travels in the diffuse double layer region between clay platelets and experiences a long range positive electrostatic interaction with the negatively charged clay surface. This positive interaction is strong enough to increase the concentration of mobile species in the interlayer region, but too weak to localize the complex. This leads to an overall greater flux of material across the film (Figure 1B) as com-

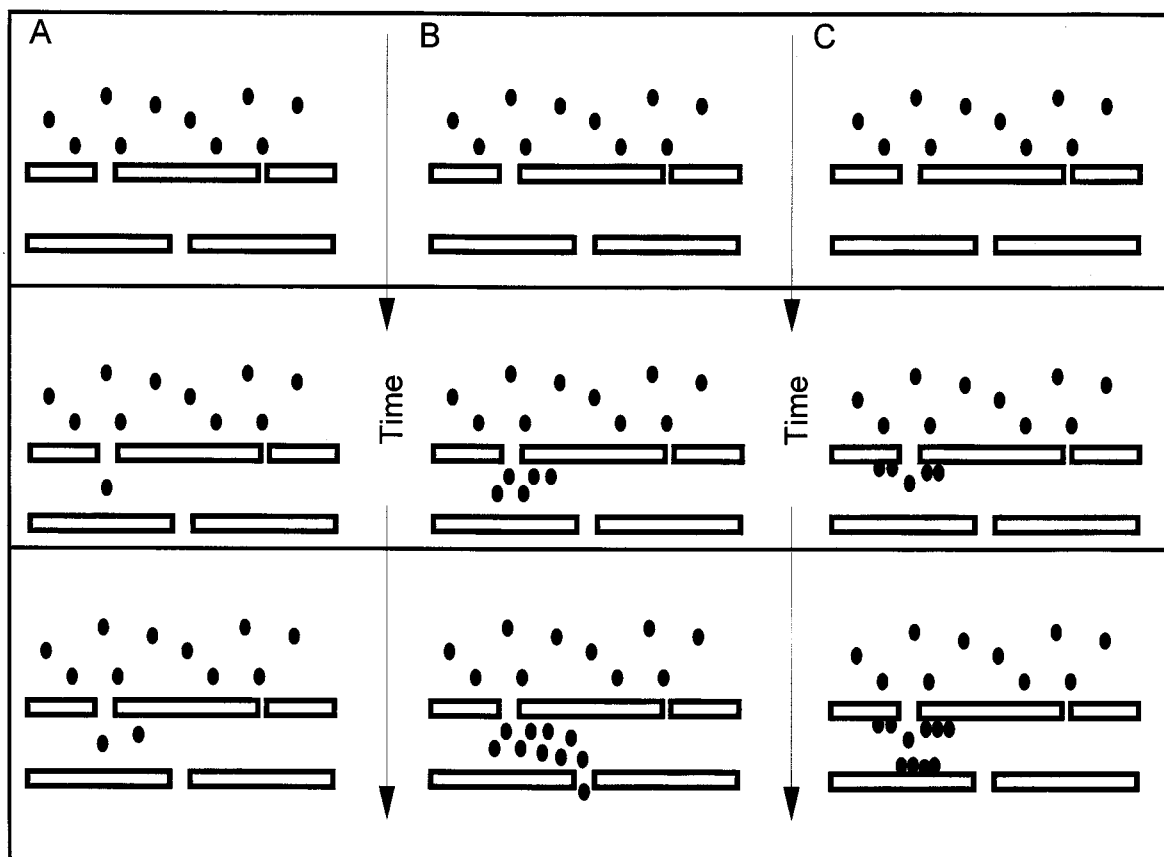


Figure 1. Well oriented clay film. A) Non-interacting molecule moves as a void filler in the interlayer region. B) Case I molecules moves in the interlayer region where its concentration is enhanced in the overlapping diffuse double layers. C) Case II molecule is adsorbed to the channel surface reducing the concentration of the mobile species.

pared to a non-interacting, void filling, solute (Figure 1A).

For Case II, the other extreme, the molecule moves from the diffuse double layer to the surface of the clay. The molecule is localized at the clay surface by either van der Waals forces (adsorbate-adsorbate or adsorbate-clay) or by hydrophobic forces. Diffusion of these molecules is controlled by equilibrium with the surface (Figure 1C). After all adsorbate sites on the clay are filled, the clay surface charge is shielded and electrostatic effects are mitigated. Under these conditions, diffusion through the film is controlled by the porosity and the concentration gradient across the film (Figure 1A).

To study these two extreme cases, and the continuum between the two, we use a series of cationic electroactive probes at CME. In this technique, the diffusive transport through an individual particle of clay can be mimicked (Fitch et al. 1995).

MATERIALS AND METHODS

KBr, NaCl, ethylenediaminetetraacetic acid, disodium salt dihydrate, Na₂EDTA, and Co(sepul-

chrate)Cl₃ (Co(sep)) (Aldrich), Ru(NH₃)₆Cl₃ and Co(ethylenediamine)₃Cl₃ (Co(en)₃³⁺) (Alfa-Aesar), and Co(NH₃)₆Cl₃ (Johnson Matthey) were used as received. Co(bipyridine)₃(ClO₄)₃ (Co(bpy)₃³⁺) was synthesized as previously described (Fitch and Lee 1993).

SWy-1 clay was obtained from the Source Clay Repository (Department of Geology Rolla, MO). The clay was suspended in deionized water, stirred overnight, centrifuged at 3500 rpm for 35 min. The supernatant was collected and freeze-dried. The freeze-dried sample was suspended at 35 g/liter in deionized water. This gel, 1 μl, was placed on an upended glass sheathed Pt electrode (0.5 mm radii). The electrode was oven dried for 10 min at 90 °C. The CME was transferred to a N₂-purged NaCl solution and the film swollen over a 5 min period. It was next transferred to a N₂-purged salt solution containing the appropriate complex. For metal complex concentrations >1 mM, multisweep cyclic voltammetry (MSCV) was immediately initiated. For complex concentration <1 mM, solutions were stirred overnight and MSCV were initiated after 12 h of equilibration in the complex containing solution.

Cyclic voltammetry (CV) was performed in a standard three electrode cell with Pt working and counter electrodes and an SCE reference electrode. A PAR potentiostat/galvanostat 273 was used with a Houston 2000 XY chart recorder. Scans were 0.4 to -0.4 V for $\text{Ru}(\text{NH}_3)_6^{3+}$, 0.4 to -0.8 V for $\text{Co}(\text{en})_3^{3+}$, 0.2 to -0.8 V for $\text{Co}(\text{sep})^{3+}$ and 0.6 to -0.2 for $\text{Co}(\text{bpy})_3^{3+}$. The scan rate was 50 mV/s.

Cation exchange capacity (CEC) displacement studies were performed by mixing 0.1 g of freeze-dried clay with 2 M of each metal complex and stirred 30 min. The clay was washed with deionized (DI) water to remove the excess metal complex. The clay was next treated with Na^+ to displace the metal complex. Solutions of displaced metal complex were analyzed on an HP 8452 Diode Array UV spectrophotometer with standard curves at 276, 210, 236 and 208 nm for $\text{Ru}(\text{NH}_3)_6^{3+}$, $\text{Co}(\text{en})_3^{3+}$, $\text{Co}(\text{sep})^{3+}$ and $\text{Co}(\text{bpy})_3^{3+}$. Mg^{2+} CEC measurements were carried out with a Mg EDTA titration.

IR studies were carried out by reacting 1 mM of each metal complex with 0.01 g of SWy-1 clay for 24 h, centrifuged, and air-dried. The dried exchanged clay was ground with KBr and observed on a ATI Mattson Genesis Series FTIR spectrometer. The spectrum of clay was subtracted from that of complex plus clay to give the spectrum of the metal complex within the clay for comparison to a pure metal complex sample.

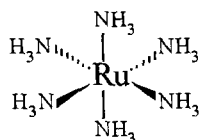
UV-Vis studies were prepared by reacting 10 mM of each metal complex with 0.5 g of SWy-1 clay in 5 ml of DI. The lower amount of clay was used to retain the gel in suspension. Spectra were acquired from 180 to 700 nm, with the majority of peaks observed at <400 nm. A difference spectrum [(Clay + metal complex)-clay] is reported and compared with the spectrum for the aqueous metal complex.

RESULTS

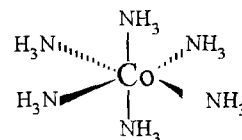
Electrochemistry

Five trivalent molecules were investigated (Figure 2). $\text{Ru}(\text{NH}_3)_6^{3+}$ was used for most of the electrochemical studies as an analog for $\text{Co}(\text{NH}_3)_6^{3+}$ because of the extreme lability of the cobalt complex upon reduction. The other three cobalt complexes increase in number of bonds and atoms while maintaining an octahedral coordination with C, H linkages between N ligands. These metal complexes were categorized as Case I or Case II based on their electrochemistry. Case I molecules moving in the diffuse double layer region (center of an uncoated clay interlayer region) may be distinguished from Case II molecules by several features.

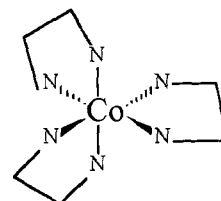
The first features are the negative shift in potential of Case I molecules and the potential dependence on sodium concentration (Naegeli et al. 1986; Fitch 1990a). The shift in potential is related to the exchange



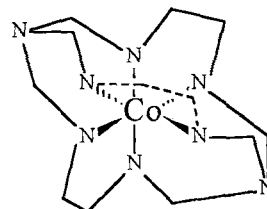
0.264 nm



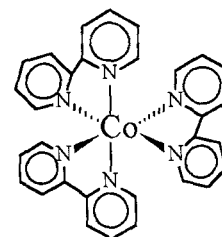
0.25 nm



0.372 nm



0.383 nm



0.586 nm

Figure 2. Probe molecules used in this study: A) $\text{Ru}(\text{NH}_3)_6^{3+}$; B) $\text{Co}(\text{NH}_3)_6^{3+}$; C) $\text{Co}(\text{en})_3^{3+}$; D) $\text{Co}(\text{sep})_3^{3+}$; E) $\text{Co}(\text{bpy})_3^{3+}$.

Molecular radii computed by Spartan; Brown and Sutin 1979; Doine and Swaddle 1991; Szalda et al. 1983.

constants of the oxidized (K_{ox}) and reduced (K_{red}) species with the clay and the solution redox potential of the complex (Table 1):

$$E_{\text{clay}}^{\circ} = \frac{-\Delta G_{\text{rx}}}{F} = E_{\text{soln}}^{\circ} - \frac{RT}{nF} \ln(K_{\text{ox}}/K_{\text{red}}) \quad [1]$$

For simple diffuse double layer exchange, the equi-

Table 1. Reactions and their energetic relationships.

Reaction	K or E	ΔG
$M^{3+} + e \rightleftharpoons M^{2+}$	E_{soln}°	$-FE_{\text{soln}}^{\circ}$
$M^{3+}X_3 + 3Na^+ \rightleftharpoons M^{3+} + 3NaX$	$1/K_{\text{ox}}$	$-RT \ln(1/K_{\text{ox}})$
$M^{2+} + 2NaX \rightleftharpoons M^{2+}X_2 + 2Na^+$	K_{red}	$-RT \ln(K_{\text{red}})$
$M^{3+}X_3 + e + Na^+ \rightleftharpoons M^{2+}X_3 + NaX$	E_{clay}°	$-FE_{\text{soln}}^{\circ} - RT \ln(K_{\text{red}}/K_{\text{ox}})$

librium constant for the reaction of a species j with a surface is:



and has been given as (Stahlerg 1994):

$$K = X_{js}/(X_j X_s \exp(-z_j F \psi_o / RT)) \quad [3]$$

where X_{js} is the fraction of occupied surface sites and X_s is the fraction of unoccupied surface sites, X_j is the mole fraction of counterions in the bulk phase, z_j is the charge on the species j and ψ_o is the potential of the surface. Equation [3] predicts that K increases exponentially with increasing z . For our trivalent probe, molecules $z_{\text{ox}} = 3$ and $z_{\text{red}} = 2$. Consequently, clay stabilizes the oxidized species resulting in a negative shift in the potential (Equation [1]).

Figure 3 illustrates typical cyclic voltammograms for some of the redox species at the bare electrode and at the CME. For $\text{Ru}(\text{NH}_3)_6^{3+}$, $\text{Co}(\text{NH}_3)_6^{3+}$, $\text{Co}(\text{en})_3^{3+}$ and $\text{Co}(\text{sep})^{3+}$, the peak for reduction is observed at a more negative potential than at the bare electrode. The negative shift is consistent with the electrostatic (Equations [1], [2] and [3]) uptake of Case I. For $\text{Co}(\text{bpy})_3^{2+}$ the potential is shifted positive indicating that the divalent form is stabilized more than the trivalent form. This suggests a hydrophobic mode of localization of the metal complex.

The observed potential for an electrostatically retained species will also depend upon the concentration of Na^+ in the bathing solution (Naegeli et al. 1986). This dependence is due to a competition between the metal complex and Na^+ for exchange sites (Table I). The Nernst equation for the overall reaction is written as:

$$E = E_{\text{clay}}^{\circ} + \frac{RT}{nF} \ln \frac{[\text{Na}^+]}{[\text{NaX}]} - \frac{RT}{nF} \ln \frac{[\text{M}^{2+}X_2]}{[\text{M}^{3+}X_3]} \quad [4]$$

Equation [4] tells us that when half of the metal complex is reduced and half is oxidized, the applied po-

tential, E , is equivalent to the first two right-hand side terms. In practice, this term can be measured in a cyclic voltammetric experiment by the midpoint between the reduction and oxidation peaks. An estimate of this potential is given either by one of the peak potential. Equation [4] indicates that the observed mid peak potential depends upon the ratio of the exchange constants, embodied in E_{clay}° (Equation [1]), the number of sites already occupied, $[\text{NaX}]$ and the competing cation concentration, $[\text{Na}^+]$.

For a single experiment in which Na^+ is in excess and therefore constant, there should be constant shift positive in potential as $[\text{NaX}]$ decreases with metal complex uptake. Such a shift is seen, with $\text{Co}(\text{sep})^{3+}$ and $\text{Co}(\text{en})_3^{3+}$ as good examples (Figure 3). Note for $\text{Co}(\text{sep})^{3+}$ as the film fills the currents increase and the potential, initially very negative, shifts positive. For $\text{Co}(\text{en})_3^{3+}$ the peaks represent a time sequence which both follows filling and subsequent loss of the signal. At the beginning of the filling sequence, the peak is shifted negative and moves positive as the signal increases. Upon loss of the signal, the peak shifts negative. These potential changes are consistent with changes in $[\text{NaX}]$.

Equation [4] indicates that an electrostatically held metal complex should have a potential dependence on $[\text{Na}^+]$ with a slope of $25.7 \text{ mV}/\ln[\text{Na}^+]$. Figure 4 illustrates that the potentials of the maximum observed peaks for $\text{Ru}(\text{NH}_3)_6^{3+}$, $\text{Co}(\text{en})_3^{3+}$ and $\text{Co}(\text{sep})^{3+}$ shift positive as a function of $\ln[\text{Na}^+]$. Slopes determined from all four points are $24.4 \text{ mV}/\ln[\text{Na}^+]$ for $\text{Ru}(\text{NH}_3)_6^{3+}$, $25.8 \text{ mV}/\ln[\text{Na}^+]$ for $\text{Co}(\text{en})_3^{3+}$ and $18 \text{ mV}/\ln[\text{Na}^+]$ for $\text{Co}(\text{sep})^{3+}$. Such a shift confirms the Case I assignment of these molecules. In contrast, the $\text{Co}(\text{bpy})_3^{3+}$ couple shows a small negative dependence upon $\ln[\text{Na}^+]$ (slope of $-5.9 \text{ mV}/\ln[\text{Na}^+]$). The direction and magnitude of the potential dependence is inconsistent with an electrostatic mode of uptake. In Case II (hydrophobic or van der Waals) uptake, there

Table 2. Mole of ion in rinse.

Rinse	Mg^{2+}	$\text{Ru}(\text{NH}_3)_6^{3+}$	$\text{Co}(\text{NH}_3)_6^{3+}$	$\text{Co}(\text{en})_3^{3+}$	$\text{Co}(\text{sep})^{3+}$	$\text{Co}(\text{bpy})_3^{3+}$
1	0.0255	0.014	0.01602	0.00538	0.0019	0.0021
2	0.0073	0.01	0.00561	0.00438	0.0005	0.00016
3	0.0034	0.004	0.00181	0.00138	0.0003	0.00004
Total	0.0362	0.028	0.02344	0.01014	0.0027	0.0023
CECL meq/g	0.724	0.84	0.7032	0.3042	0.078	0.069

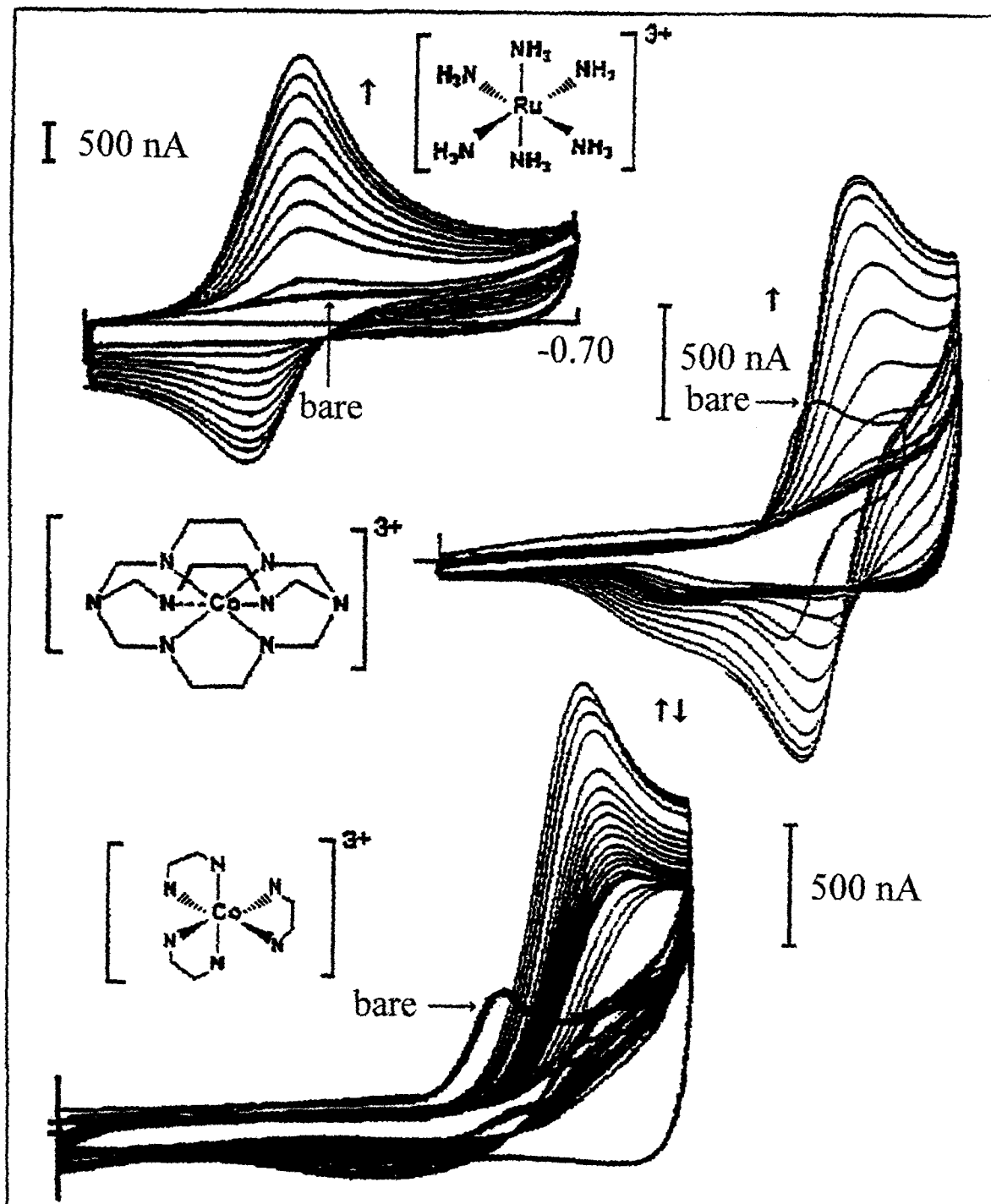


Figure 3. Multisweep cyclic voltammograms (MSCV) for SWy-1 (CME) obtained at 50 mV/s. A) $0.01 \text{ mM Ru(NH}_3)_6\text{Cl}_3$, $0.01 \text{ M Na}_2\text{SO}_4$, potential swept between 0 and 0.7 V vs SCE. Scale is 500 nA. B) $0.5 \text{ mM Co(sep)Cl}_3$ in 0.1 M NaCl , potential swept between 0.1 and -0.85 V vs SCE . Scale is 500 nA. C) $0.5 \text{ mM Co(en)}_3\text{Cl}_3$, potential swept between 0.3 and -0.85 V vs SCE . Scale is 500 nA. The single sweep, time invariant, signal for the bare electrode is indicated.

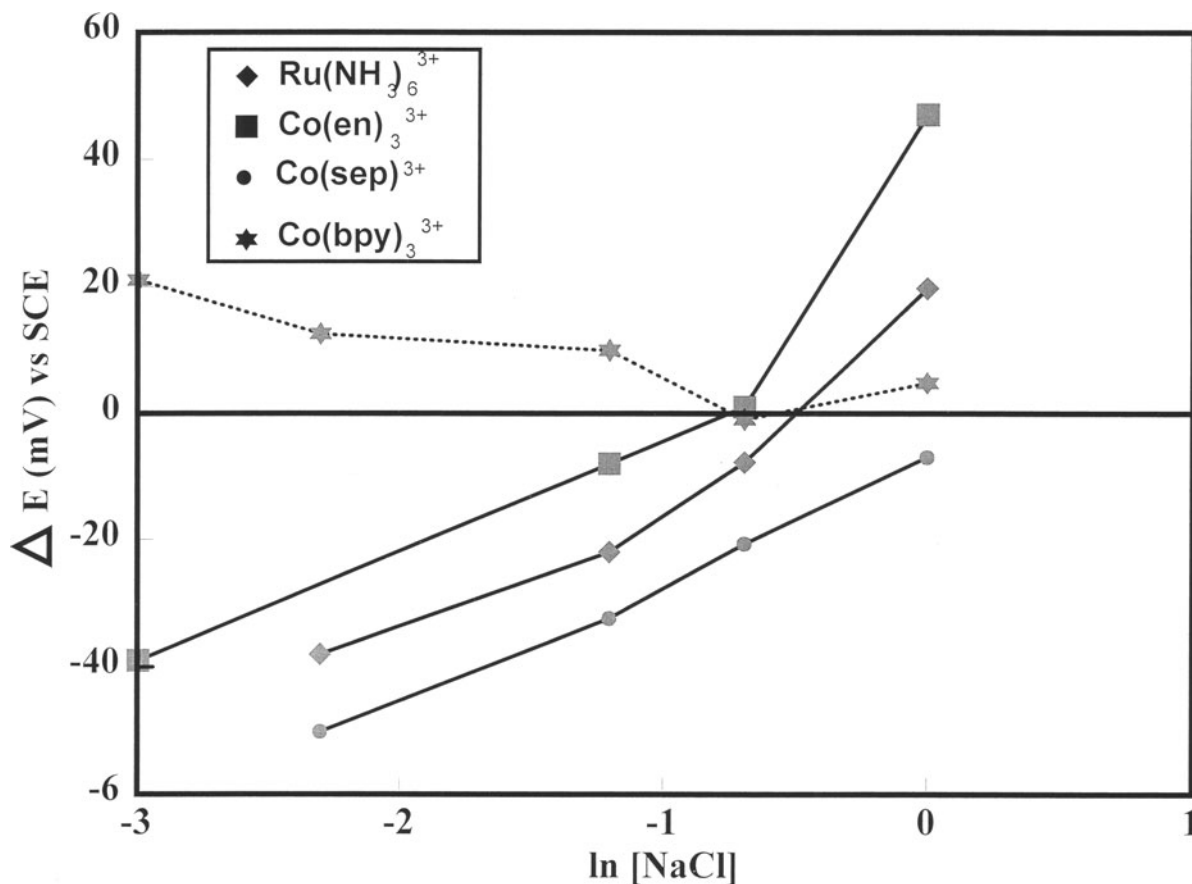


Figure 4. Potential dependence ($\Delta E = E_{\text{CME}}^{\circ} - E_{\text{bare}}^{\circ}$) of various redox couples (1 mM), measured at steady state, at a CME as a function of NaCl concentration.

is no Na^+ participation in the uptake process. Therefore $\text{Co}(\text{bpy})_3^{3+}$ is classified as a Case II complex.

The cyclic voltammograms in Figure 3 indicate that $\text{Ru}(\text{NH}_3)_6^{3+}$, $\text{Co}(\text{en})_3^{3+}$ and $\text{Co}(\text{sep})_3^{3+}$ at the CME have currents that at some point in time are greatly enhanced over the currents obtained at the bare electrode. In contrast, the current for $\text{Co}(\text{bpy})_3^{3+}$ at the CME only exceeds the bare electrode current at low bulk solution concentrations of the metal complex. This differential behavior contains information about the mode of uptake and transport.

The peak current at a clay-modified electrode is described by (Fitch et al. 1995):

$$I_p = 2.69 \times 10^5 n^{3/2} (d\Sigma b) (\tau D_{\text{clay}})^{1/2} \kappa C_{\text{bulk}} \quad [5]$$

where n is the number of electrons involved in the oxidation/reduction reaction at the electrode surface, $(d\Sigma b)$ is the interlayer area available for charge transport defined by the b dimension of the clay and the interlayer spacing ∂ , τ is a tortuosity factor accounting for the movement lateral to the concentration gradient imposed by the platelike structure, D_{clay} is the clay diffusion coefficient assumed to apply within the clay

film, κ is the partition coefficient between the clay solution and the bulk solution and C_{bulk} is the concentration of the electroactive probe within the bathing solution.

When the current at the clay-modified electrode is normalized by the current at the bare electrode one obtains:

$$R = (\tau^{1/2} \partial \Sigma b / A) (D_{\text{clay}} / D_{\text{soln}})^{1/2} \kappa \quad [6]$$

where D_{soln} is the aqueous solution diffusion coefficient of the complex and A is the area of the underlying electrode. Experimentally, $\tau^{1/2} \partial \Sigma b / A$ is a constant and can be estimated from the transport of an un-retained complex where κ is 1 (Fitch and Fausto 1988). For an SWy-1 clay-modified electrode swollen in 0.02 M NaCl, this term is usually close to 0.5. Therefore, the differences in currents between $\text{Ru}(\text{NH}_3)_6^{3+}$, $\text{Co}(\text{en})_3^{3+}$, $\text{Co}(\text{sep})_3^{3+}$ and $\text{Co}(\text{bpy})_3^{2+}$ must relate to $(D_{\text{clay}} / D_{\text{soln}})^{1/2} \kappa$. If we postulate that D_{soln} and κ are similar, then the main variable between metal complexes is D_{clay} . We suggest that Case I complexes move with a solution diffusion coefficient within the diffuse double layer region of the interlayer while Case II metal

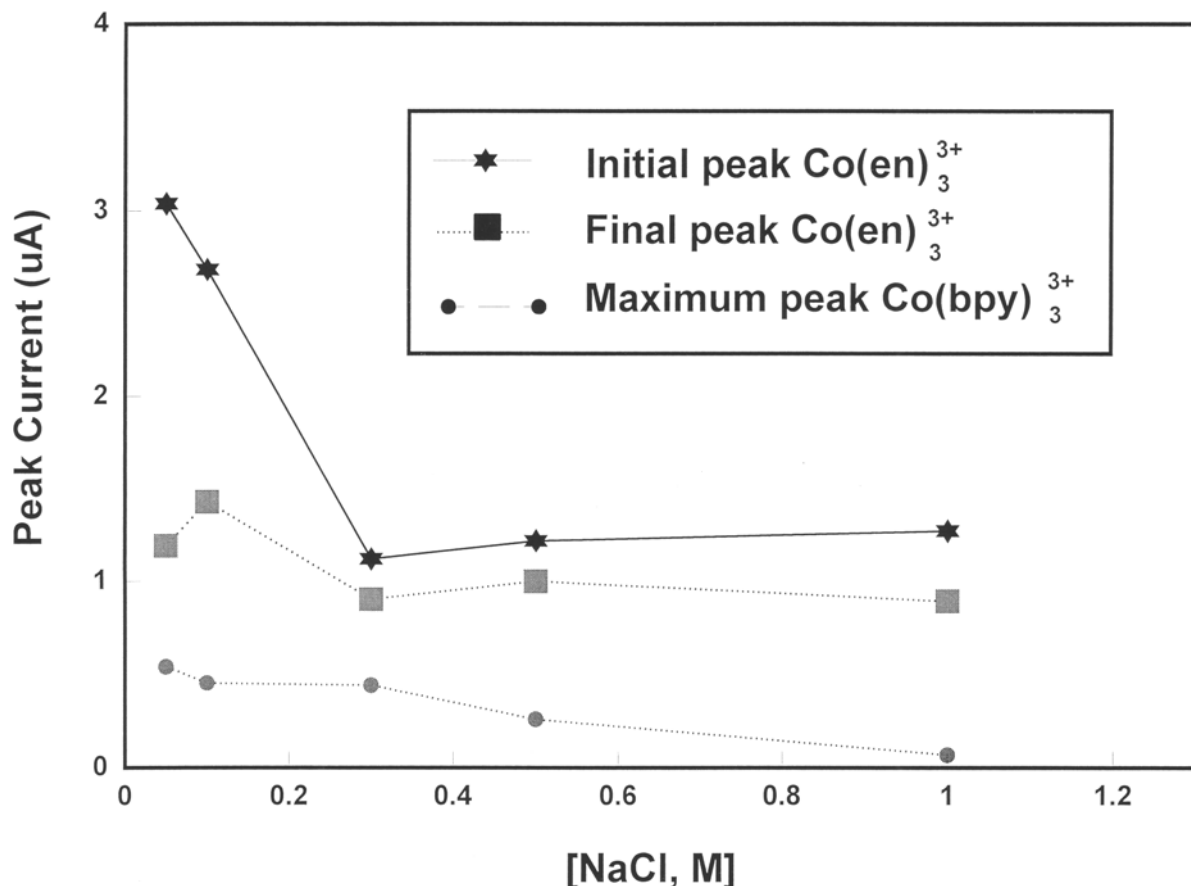


Figure 5. Peak currents as a function of [NaCl] for the first observed peak of 1 mM $\text{Co(en)}_3\text{Cl}_3$, its final steady state peak, and the maximum observed peak of 1 mM $\text{Co(bpy)}_3(\text{ClO}_4)_3$ at CME in 0.1 M NaCl.

complexes are surface adsorbed and move with a surface diffusion coefficient.

This hypothesis can be tested. A surface diffusing species will be less sensitive to the interlayer dimension than a species diffusing in the diffuse double layer between two clay platelets. Consequently, variation in δ will be expected to play an important role in the magnitude of the observed currents for the Case I metal complexes ($\text{Ru}(\text{NH}_3)_6^{3+}$, Co(en)_3^{3+} and Co(sep)^{3+} as compared to Co(bpy)_3^{3+} . The interlayer dimension in these experiments is controlled by the Na^+ concentration of the swelling solution (Fitch and Fausto 1988; Lee and Fitch 1990; Fitch et al. 1995). At 0.3 M Na^+ , the films change abruptly from an approximate 10 Å interlayer dimension to an approximate 60 Å interlayer dimension. This abrupt change distinguishes the interlayer swelling effect of Na^+ from its competitive ion effect.

Figure 5 illustrates the difference between a Case I (Co(en)_3^{3+}) and Case II (Co(bpy)_3^{3+}) complex when the clay films are initially swollen in different Na^+ concentrations. Co(en)_3^{3+} shows an abrupt change in maximum peak height at the expected Na^+ concentra-

tion, while Co(bpy)_3^{3+} is relatively insensitive to Na^+ concentration. This is consistent with a surface transport mechanism for Co(bpy)_3^{3+} and an initial interlayer diffusion mechanism for Co(en)_3^{3+} .

For Case I molecule Co(en)_3^{3+} , the peak current decays with time (Figure 1). This loss of activity can be caused by loss of the metal complex from the clay to the solution or by chemical transformation and/or conversion of the metal complex from an interlayer species to a surface species. Since the bulk solution contains an excess of the metal complex, leaking is unlikely. Chemical transformations may occur. The most obvious transformations are the ligand substitution reactions of Co(en)_3^{2+} and $\text{Co}(\text{NH}_3)_6^{2+}$ divalent complexes (Fischer and Bezdek 1973; Mayer et al. 1979; Sahami and Weaver 1981). These are apparent from the smaller oxidation (as compared to reduction) peaks observed at both the clay-modified and bare electrodes (Figure 3). This phenomena is ordinarily attributed to a chemical reaction that follows reduction. The chemical reaction reduces the concentration of the reduced species in the vicinity of the electrode and therefore diminishes the peak associated with the re-oxidation

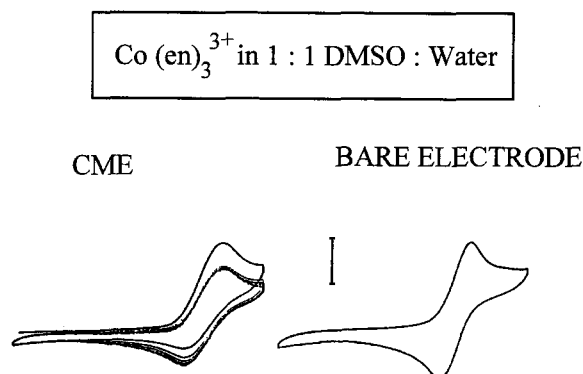


Figure 6. MSCV for 1 mM $\text{Co}(\text{en})_3\text{Cl}_3$ in 1:1 water:DMSO mixture at bare and CME. Scale is 0.5 μA . Potential limits same as in Figure 3C. Note enhanced presence of the oxidative peak at the bare as compared to the CME.

of the compound. Given the well known substitutional lability of the reduced form of this metal complex, we attribute the loss of the peak to attack of the compound by water. The ligand substitution reaction may be inhibited by addition of a non-aqueous solvent (DMSO or AN) to the solution (Figure 6). Note that while the oxidative peak is observed at the bare electrode, it is not observed at the CME in the presence of the non-aqueous solvent. This is most likely due to an exclusion of the non-aqueous solvent at the clay-modified electrode.

It is also likely that the substitutional lability of $\text{Co}(\text{en})_3^{3+}$ noted above is involved in the decay of the signal for $\text{Co}(\text{en})_3^{3+}$ at the CME over time. Substitutionally inert $\text{Co}(\text{sep})_3^{3+}$ shows no such decay (Figure 3). The final product of $\text{Co}(\text{en})_3^{3+}$ decay within the clay may or may not occupy the diffuse double layer region of the interlayer. As before, a test of its location is peak sensitivity to the interlayer dimension. Figure 5 indicates that the initial interlayer dimension dependent, electrostatic interaction, of $\text{Co}(\text{en})_3^{3+}$ with the clay is superseded by a surface associated, interlayer dimensions independent form. This suggests that the final form of the metal complex observed will be difficult to rinse from the clay, as was observed. In contrast, $\text{Ru}(\text{NH}_3)_6^{3+}$ can be released from clay with this rinse cycle (Wieglos and Fitch 1990).

Supporting Studies

The electrochemical data suggest that $\text{Ru}(\text{NH}_3)_6^{3+}$ interacts primarily via long range electrostatic forces felt within the overlapping diffuse double layers of two clay platelets. $\text{Co}(\text{en})_3^{3+}$ and $\text{Co}(\text{sep})_3^{3+}$ are intermediate type species that show an observable electrostatic component in uptake, followed in time by a non-electrostatic retention mechanism. $\text{Co}(\text{bpy})_3^{3+}$ is observed only in its non-electrostatic state. These results are confirmed by a displacement study (Table 2). A standard method for determining the CEC of a clay is

to saturate all sites with Mg^{2+} , rinse, displace Mg^{2+} with a competitive cation (for example, Na^+) and measure Mg^{2+} in the displaced solution. From this procedure, the CEC is determined to be 0.72 meq/g, consistent with literature values (Van Olphen 1979). This value is approached by displacement of $\text{Co}(\text{NH}_3)_6^{3+}$ (CEC of 0.7 meq/g) and $\text{Ru}(\text{NH}_3)_6^{3+}$ (CEC of 0.84 meq/g) but not by $\text{Co}(\text{en})_3^{3+}$ (0.26 meq/g), $\text{Co}(\text{sep})_3^{3+}$ (0.078 meq/g) or $\text{Co}(\text{bpy})_3^{3+}$ (0.069 meq/g). For the latter three species, very little of the adsorbed metal complex is displaced by Na^+ . The value for $\text{Co}(\text{bpy})_3^{3+}$ is consistent with that obtained for $\text{Ru}(\text{bpy})_3^{2+}$ hectorite (0.07 meq/g) (Krenske et al. 1980).

Supporting UV-Vis and IR studies were performed with $\text{Ru}(\text{NH}_3)_6^{3+}$, $\text{Co}(\text{en})_3^{3+}$, $\text{Co}(\text{sep})_3^{3+}$ and $\text{Co}(\text{bpy})_3^{3+}$. For all metal complexes, substantial decrease and shifts of N-H vibrations are observed: 3423–3565 (Sastri 1965; Ugo and Gillard 1967); 3040 (Gahan et al. 1989); 1316 and 1612 (Allen and Senoff 1967); and 1320 and 780 cm^{-1} (Earley and Fealey 1973). This is consistent with the dried state of the sample and the close proximity of the hydrogen in the N-H bond to the clay surface. Of particular significance in these spectrum are the metal-ligand vibrations to be found in the 420–500 cm^{-1} region (Earley and Feeley). Perturbation of this vibration increases through the sequence $\text{Ru}(\text{NH}_3)_6^{3+} \rightarrow \text{Co}(\text{bpy})_3^{3+}$. For $\text{Ru}(\text{NH}_3)_6^{3+}$, the metal-ligand vibration is unperturbed (466.68 cm^{-1}). For $\text{Co}(\text{en})_3^{3+}$, the vibration is sharpened and shifted to a long wavelength (470.54 to 464.76 cm^{-1}). For $\text{Co}(\text{sep})_3^{3+}$, three vibrations in this region (534.18, 451.26 and 404.97 cm^{-1}) shift and converge into two vibrations (501.4 and 464.76 cm^{-1}). Finally, for $\text{Co}(\text{bpy})_3^{3+}$, bands at 478.25 and 420.40 cm^{-1} are diminished and observed at 501.40 and 462.83 cm^{-1} . The important point to note is that the metal complex that has been identified as having a long range electrostatic (CEC) interaction with the clay, $\text{Ru}(\text{NH}_3)_6^{3+}$, exhibits no shifts in the M-L vibration.

The UV-Vis spectra for the free metal complex and the metal complex in the clay (clay contribution subtracted) indicate no significant changes with the striking exception of $\text{Co}(\text{sep})_3^{3+}$. Adsorption of the metal complex by the clay converts a multipeak spectrum (210, 234 and 256 nm) into a very broad and featureless spectrum centered at 234 nm. This may be indicative of major solvation changes of the metal complex within the clay. For $\text{Ru}(\text{NH}_3)_6^{3+}$, no changes are noted in the spectrum initially but extended aging results in the development of Ru red (Fletcher et al. 1961) consistent with the observed reaction of $\text{Ru}(\text{NH}_3)_6^{3+}$ on silica after long time periods (Ramaraj and Kaneko 1993).

DISCUSSION

Figure 2 gives estimated radii of the metal complexes. The Case II character of the molecules is pro-

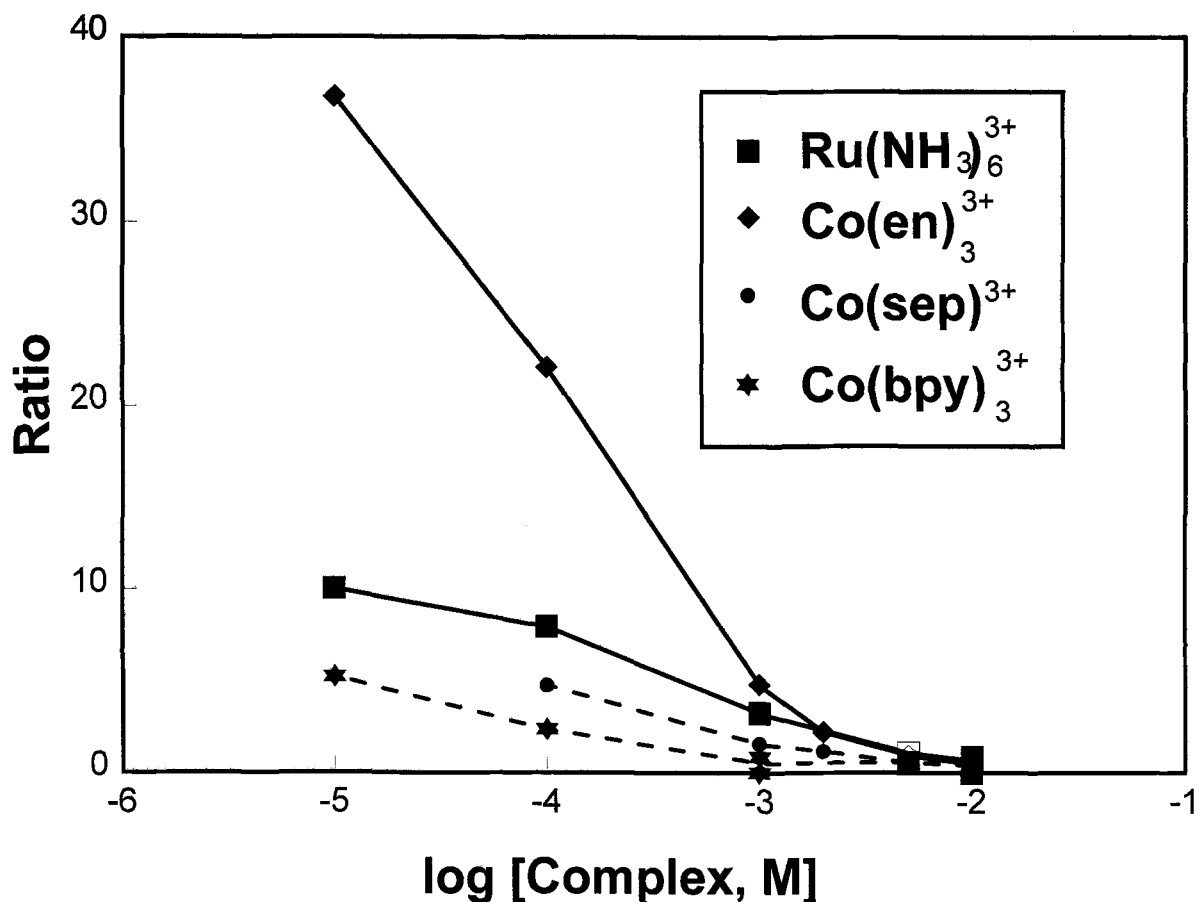


Figure 7. Current enhancement plotted as Ratio (Ratio = $I_{p,CME}/I_{p,bare}$) as a function of the bathing solution concentration of the complex in 0.1 M NaCl.

portional with the number of atoms but not with the radii. This indicates that a molecular sieving selection mechanism has little effect on the retention of the metal complexes.

All metal complexes are octahedrally coordinated with N as the electron donor. The Case I metal complex, $\text{Co}(\text{NH}_3)_6^{3+}$, has been previously determined to stoichiometrically exchange at Na^+ exchange sites in clay (Fripiat and Helsen 1966). $\text{Co}(\text{en})_3^{3+}$ has also been implicated in simple cation exchange (Kanungo et al. 1973) and was found to orient with its 3-fold axis perpendicular to the clay surface (Kaneyoshi et al. 1993). In contrast, the electrochemical experiments shown here suggest that addition of the 6 carbons in $\text{Co}(\text{en})_3^{3+}$, results in a substantially decreased observable electrostatic mechanism relative to $\text{Co}(\text{NH}_3)_6^{3+}$. This observation is consistent with that made by Knudsen and McAtee (1973) who suggested that $\text{Co}(\text{en})_3^{3+}/\text{Na}^+$ exchange with clay was not solely electrostatic in nature. The non-electrostatic retention of the complexes may occur via H-bonding (Cloos and Lauro 1972) or via substitution of ligands by the clay surface as is observed for $\text{Cu}(\text{en})_2^{2+}$ (Burba and

McAtee 1977). Surface substitution for axial ligands results in an increase of the crystal field stabilization energy for $\text{Cu}(\text{en})_3^{2+}$ (Velghe et al. 1977; Maes et al. 1980).

$\text{Co}(\text{sep})_3^{3+}$ and $\text{Co}(\text{en})_3^{3+}$ differ only in the presence of two additional C chain bridges in the former. The increase in number of carbon atoms once again results in a final retention mechanism that is increasingly non-electrostatic. $\text{Co}(\text{sep})_3^{3+}$ retention within the clay can not proceed via ligand substitution due to the inertness of the complex (Endicott et al. 1982; Ebersson and Ekstrom 1988). However, the metal complex does have a measurable pK_a associated with N-H bonds. Furthermore, the metal complex participates in proton transfer reactions (Bakava et al. 1983). Thus, hydrogen bonding as a means of localization is possible. An alternative retention mechanism is also possible. The metal complex strongly ion pairs, via hydrophobic mechanisms, with a wide range of anions to form clusters (Sotomayor et al. 1991; Indelli and Duatli 1986). Such cluster formation could be facilitated within the interlayer, as was surmised for trisbipyridine complexes (Fitch and Edens 1989). It is interesting to note that

despite strong retention of $\text{Co}(\text{sep})^{3+}$, the electrochemical signal is not as suppressed as for $\text{Co}(\text{bpy})_3^{3+}$. The larger current and negative potential of the retained species suggest an accessible interlayer localized species.

Despite changes in their retention mechanism, neither $\text{Co}(\text{en})_3^{3+}$ or $\text{Co}(\text{sep})^{3+}$ exhibit the extreme Case II behavior of $\text{Co}(\text{bpy})_3^{3+}$. $\text{Co}(\text{bpy})_3^{3+}$ is strongly adsorbed by montmorillonite (6.9 meq/100g) and hectorite (7 meq/100g) (Krenske et al. 1980) as evidenced by low exchangeability relative to the CEC. Further evidence of a non-electrostatic mode of uptake is adsorption in excess of the CEC with subsequent charge reversal for the clay (Swartzen-Allen and Matijevic 1975). We conclude that the aromatic ring on $\text{Co}(\text{bpy})_3^{3+}$ plays an important role in the hydrophobicity of the metal complex.

These results have implications for both the development of sensor or charge storage devices and for the diffusive transport of materials in natural environments (landfills). For sensors, one hopes to obtain larger electrochemical signals through the use of the clay films at electrode surfaces. For Case I molecules, enhanced signals over a wide range of concentrations can be obtained (Figure 7).

For charge storage devices, the localized species must remain electrochemically accessible. This requirement has defeated the practical use of trisbipyridine complexes in clay-modified electrodes due to the minimal accessibility of the localized species. The finding that $\text{Co}(\text{sep})^{3+}$ is localized and remains electrochemically accessible has significant implications to the design of such devices.

Transport in the natural environment is seen to be a complex interplay of electrostatic and hydrophobic forces. Highly soluble cationic species are expected to have diffusion coefficients nearly equal to those observed in aqueous media. This high diffusion coefficient combined with a high concentration of the complex in the diffuse double layer results in a large mobility of these complexes in clays. Examples of this class of molecules are $^3\text{H}^+$ and NH_4^+ .

ACKNOWLEDGEMENTS

This work was supported by NSF CHE-9017273 and NSF CHE-9315396.

REFERENCES

- Allen AD, Senoff CV. 1967. Preparation and infrared spectra of some ammine complexes of Ruthenium(II) and Ruthenium(III). *Can J Chem* 45:1337–1341.
- Bakava A, Espenson JH, Creaser II, Sargeson AM. 1983. Kinetics of the superoxide radical oxidation of [Cobalt sepulchrate](2+). A flash photolytic study. *J Am Chem Soc* 105:7264–7268.
- Barone FS, Yanful EK, Quigley RM, Row RK. 1989. Effect of multiple contaminant migration on diffusion and adsorption of some domestic waste contaminants in a natural clayey soil. *Can Geotech J* 26:189–198.
- Burba III JL, McAtee JL, Jr. 1977. The orientation and interaction of ethylenediamine Copper(II) with Montmorillonite. *Clays & Clay Miner* 25:113–118.
- Brown GM, Sutin N. 1979. A comparison of the rates of electron exchange reactions of ammine complexes of Ruthenium(II)–(III) with the predictions of the adiabatic, outer-sphere electron transfer models. *J Am Chem Soc* 101:883–892.
- Cloos P, Lauro RD. 1972. Adsorption of Ethylenediamine (EDA) on Montmorillonite saturated with different cations II. Hydrogen—and ethylenediammonium—Montmorillonite and hydrogen bonding. *Clays & Clay Miner* 20:259–270.
- Crooks VE, Quigley RM. 1989. Saline leachate migration through clay: A comparative laboratory and field investigation. *Can J Geotech* 21:349–362.
- Doine H, Swaddle TW. 1991. Pressure effects on the self-exchange rates of Cobalt(III/II) couples. Evidence for adiabatic electron transfer in the Bis(1,4,7-trithiacyclononane) and Sepulchrate Complexes. *Inorg Chem* 30:1858–1862.
- Earley JE, Fealey T. 1973. Hydroxide ion as a reducing agent for cations containing three ruthenium atoms in nonintegral oxidation states. *Inorg Chem* 12:2, 323–327.
- Eberson I, Ekstrom M. 1988. Electron transfer reactions in organic chemistry. XIV. The reactivities of some polyalcanes toward the outer sphere electron transfer reductants $\text{Co}(\text{II})\text{sepulchrate}$ and $\text{Co}(\text{II})\text{W}_{12}\text{O}_{40}^{7-}$. *Acta Chem Scand* B42:1113–121.
- Edens GJ, Fitch A, Lavy-Feder A. 1991. Use of isopotential points to elucidate ion exchange reaction mechanisms: $\text{Cr}(\text{bpy})_3^{3+}$ at Montmorillonite clay modified electrodes. *J Electroanal Chem* 307:139–154.
- Endicott JF, Durham B, Kuma K. 1982. Examination of the intrinsic barrier to electron transfer in Hexa-aquacobalt(III). Evidence for very slow outer-sphere self-exchange resulting from contributions of Frank-Condon and electronic terms. *Inorg Chem* 21:2437–2444.
- Fischer O, Bezdek J. 1973. Study of the kinetics of electrode processes by means of electrolysis with constant current. XIX. Comparison of preceding and succeeding first order reactions. *Coll Czech Chem Comm* 38:1907–1910.
- Fitch A. 1990. Apparent formal potential shifts in ion exchange voltammetry. *J Electroanal Chem* 284:237–244.
- Fitch A. 1990. Clay-modified electrodes: A review. *Clays & Clay Miner* 38:391–400.
- Fitch A, Edens GJ. 1989. Isopotential points as a function of an allowed cross reaction. *J Electroanal Chem* 267:1–13.
- Fitch A, Du J. 1992. Diffusion layer in well ordered clay-modified electrodes. *J Electroanal Chem* 319:409–414.
- Fitch A, Du J, Gan H, Stucki JW. 1995. Effect of clay charge on swelling: A clay-modified electrode study. *Clays & Clay Miner* 43:607–614.
- Fitch A, Fausto CL. 1988. Insulating properties of clay films towards $\text{Fe}(\text{CN})_6^{3-}$. *J Electroanal Chem* 257:299–303.
- Fitch A, Lavy-Feder A, Lee SA, Kirsh MT. 1988. Montmorillonite face surface associated $\text{Cr}(\text{bpy})_3^{3+}$ monitored electrochemical: M.T. *J Phys Chem* 92:6667–6670.
- Fitch A, Lee SA. 1993. Effect of clay charge on $\text{Cr}(\text{bpy})_3^{3+}$ reaction mechanism at clay-modified electrodes. *J Electroanal Chem* 344:45–59.
- Fitch A, Subramaniam P. 1993. Dual electroactive probes of clay film chemistry. *J Electroanal Chem* 362:177–185.
- Fletcher JM, Greenfield BF, Handy CJ, Scargill D, Woohead JL. 1961. Ruthenium Red. *J Chem Soc A* 2000.
- Fripiat JJ, Helsen J. 1966. Kinetics of decomposition of cobalt coordination complexes on montmorillonite surfaces. *Clays & Clay Miner* 14:163–9.
- Gahan LR, Healy PC, Patch GJ. 1989. Synthesis of cobalt(III) cage complexes. *J Chem Ed* 66:5, 445–446.

- Goldsmann LJ, Damle AS, Northeim CM, Greenfield LT, Kingsbury GL, Truesdale RL. 1990. Clay liners for waste management facilities: Design, construction and evaluation, pollution tech. review. #178, Noyes Data Corp. p 1-9.
- Goodall DC, Quigley RM. 1977. Pollutant migration from two sanitary landfill sites near Sarnia, Ontario. *Can Geotech J* 14:223-236.
- Indelli A, Duatli A. 1986. Association of $\text{Co}(\text{sep})^{3+}$ ions with $\text{S}_2\text{O}_3^{2-}$ ions. *J Chem Soc Farad Trans I* 82:1429-1440.
- Johnson RL, Cherry JA, Pankow JF. 1989. Diffusive contaminant transport in natural clay: A field example and implications for clay-lined waste disposal sites. *Env Sci Tech* 23:340-349.
- Kaneyoshi M, Yamagishi A, Tanaguchi M, Aramata A. 1993. Adsorption and spectroscopic studies on the interaction of cobalt(III) chelate with clays. *Clays & Clay Miner* 41:1-6.
- Kanungo JL Das, Chakravarti K. 1973. Behavior of quaternary ammonium ions in the desorption of $[\text{Co}(\text{en})_3]^{3+}$ from H-Coen3 Bentonite. *J Ind Chem Soc* 35:295-9.
- Knudson MI, Jr, McAtee JL, Jr. 1973. The effect of cation exchange of tris(ethylenediamine cobalt(III) for sodium on nitrogen sorption by montmorillonite. *Clays & Clay Miner* 21:19-26.
- Krenske D, Abdo S, Van Damme H, Cruz M, Fripiat JJ. 1980. Photochemical and photocatalytic properties of adsorbed organometallic compounds. 1. Luminescence quenching of tris(2,2'-bipyridin)ruthenium(II) and -chromium(III) in clay membranes. *J Phys Chem* 84:2447.
- Lee SA, Fitch A. 1990. Conductivity of clay-modified electrodes: Alkali metal cation hydration and film preparation effects. *J Phys Chem* 94:4998-5004.
- Maes A, Schoonheydt RA, Cremers A, Uytterhoeven JB. 1980. Spectroscopy of $\text{Cu}(\text{en})_2^{2+}$ on clay surfaces. Surface and charge density effects. *J Phys Chem* 84:2795-2799.
- Mayer U, Kotocova A, Gutmann V, Gerger W. 1979. Outer-sphere effects on the redox properties of the system $\text{Co}(\text{en})_3^3/\text{Co}(\text{en})_3^{2+}$. *J Electroanal Chem* 100:885-883.
- Mott HV, Weber WJ, Jr. 1991. Factors influencing organic contaminant diffusivities in soil-bentonite cutoff barriers. *Env Sci Tech* 25:1708-1715.
- Naegeli R, Redepenning J, Anson FC. 1986. Influence of supporting electrolyte concentration and composition on formal potentials and entropies of redox couples incorporated in nafion coatings on electrodes. *J Phys Chem* 90:6227-6232.
- Quigley RM, Fernandez F, Yanful E, Helgason T, Margaritis A, Whitby JL. 1987. Hydraulic conductivity of contaminated natural clay directly below a domestic landfill. *Can Geotech J* 24:377-383.
- Ramaraj R, Kaneko M. 1993. In-situ spectroscopic voltammetric studies on Ru-red and Ru-brown complexes for water oxidation catalyst in homogeneous aqueous solution and in heterogeneous nafion membranes. *J Molecular Catalysis* 81:319-332.
- Sahami S, Weaver MJ. 1981. Solvent effects on the kinetics of simple electrochemical reactions. Part I. Comparisons of the behavior of $\text{Co}(\text{III})/(\text{II})$ trisethylenediamine and ammine couples with the predictions of dielectric continuum theory. *J Electroanal Chem* 124:35-51.
- Sastri VS. 1972. Studies on the disposition of carbonato group in cobalt(III) complexes. *Inorg Chim Acta* 6:2, 264-266.
- Sotomayor J, Santos H, Pina F. 1991. Application of ^{59}Co NMR to the investigation of interactions between cobalt sepulchrate and various counterions. *Can J Chem* 69:567-569.
- Stahlerg J. 1994. Electrostatic retention model for ion-exchange chromatography. *Anal Chem* 66:440-449.
- Stein JA, Fitch A. 1995. Computerized system for dual electrode multi-sweep cyclic voltammetry: Its use in clay-modified electrode studies. *Analytical Chem* 67:1322-1325.
- Subramaniam P, Fitch A. 1992. Diffusional transport of solutes through clay: Use of clay-modified electrodes. *Environ Sci Technol* 26:1775-1779.
- Swartzen-Allen SL, Matijevic E. 1975. Colloid and surface properties of clay suspensions. II. Electrophoresis and cation adsorption of montmorillonite. *J Coll Inter Sci* 50:1, 143-153.
- Szalda DJ, Creutz C, Mahajan D, Sutin N. 1983. Electron-transfer barriers and metal-ligand bonding as a function of metal oxidation state. 2. Crystal and molecular structure of tris(2,2'-bipyridine) cobalt(II) dichloride-2-water-ethanol and tris(2,2'-bipyridine) Cobalt(I) chloride-water. *Inorg Chem* 22:17, 2372-2379.
- Ugo R, Gillard RD. 1967. Adducts of coordination compounds. IV—Nitric acid adducts of ammine complexes of trivalent metals. *Inorg Chim Acta* 1:2, 311-314.
- Velghe F, Schoonheydt RA, Uytterhoeven JB, Peigner P, Lunsford JH. 1977. Spectroscopic characterization and thermal stability of copper(II) ethylene-diamine complexes on solid surface. 2. Montmorillonite. *J Phys Chem* 81:12, 1187-1194.
- Wang XQ, Thibodeaux LJ, Valsaraj KT, Relble DD. 1991. Efficiency of capping contaminated bed sediments in situ. 1. Laboratory-scale experiments on diffusion-adsorption in the capping layer. *Env Sci Tech* 25:1578-1584.
- Wielgos T, Fitch A. 1990. Clay modified electrode ion exchange voltammetry. *Electroanalysis* 2:449-454.

(Received 23 June 1994; accepted 4 August 1995; Ms. 2525)